Finding Matrix Product State Representations of Highly Excited Eigenstates of Many-Body Localized Hamiltonians

Xiongjie Yu, David Pekker, and Bryan K. Clark

Phys. Rev. Lett. **118**, 017201 — Published 3 January 2017

DOI: 10.1103/PhysRevLett.118.017201

Finding matrix product state representations of highly-excited eigenstates of many-body localized Hamiltonians

Xiongjie Yu,[1] David Pekker,[2] and Bryan K. Clark[1]

[1] *Department of Physics, University of Illinois at Urbana-Champaign, IL 61801, USA*
[2] *Pittsburgh Quantum Institute and Department of Physics and Astronomy, University of Pittsburgh, PA 15260, USA*

A key property of many-body localized Hamiltonians is the area law entanglement of even highly excited eigenstates. Matrix Product States (MPS) can be used to efficiently represent low entanglement (area law) wave functions in one dimension. An important application of MPS is the widely used Density Matrix Renormalization Group (DMRG) algorithm for finding ground states of one dimensional Hamiltonians. Here, we develop two algorithms, the Shift and Invert MPS (SIMPS) and excited state DMRG which find highly-excited eigenstates of many-body localized Hamiltonians. Excited state DMRG uses a modified sweeping procedure to identify eigenstates whereas SIMPS applies the inverse of the shifted Hamiltonian to a MPS multiple times to project out the targeted eigenstate. To demonstrate the power of these methods we verify the breakdown of the Eigenstate Thermalization Hypothesis (ETH) in the many-body localized phase of the random field Heisenberg model, show the saturation of entanglement in the MBL phase and generate local excitations.

Many-body localization (MBL) is a dynamical phase of interacting, disordered, isolated quantum systems which occurs at finite energy density [1–11]. While the ground state wave-function is the key quantity for classifying equilibrium quantum phases, the finite-energy density eigenstates are the analogous quantity for dynamical phases. MBL systems have atypical eigenstates and fail to thermalize [12–14]. Analytical arguments about MBL primarily rely on analyzing the highly excited eigenstates using either diagrammatic resummation [4–8, 15] or the real space renormalization group [16–20]. Numerically, getting interior eigenvectors using exact diagonalization (ED) requires exponential computer time and memory, and as a result these are limited to rather small (at most 22-site [21]) systems [7, 22–24]. Time evolution DMRG studies are limited by the logarithmic-in-time growth of entanglement entropy that occurs in the localized phase [25–27]. It has been recently shown that the entire spectrum of eigenstates of a MBL system can be efficiently described by a matrix product operator (MPO) [28, 29]; the best available algorithm for optimizing this MPO [30] captures features of the entire spectrum but doesn't describe individual states to high fidelity. While the bulk of MBL research has been theoretical, there has been considerable recent progress on the experimental side [31, 32]. For the first time, clear signs of the MBL transition were observed in an ultracold atom experiment [33].

In this work, we take advantage of the fact that eigenstates of many-body localized systems obey the area law [12, 34, 35] and can therefore be efficiently represented as a Matrix Product State (MPS). Historically, the density matrix renormalization group (DMRG) has been an extremely fruitful approach for optimizing the ground state MPS [36]. We develop numerical algorithms for generating a MPS representations of the excited states, and use them to test the basic properties of MBL in the regime of large one-dimensional systems that were previously inaccessible due to the limitations of ED.

The algorithms we develop fall into two broad classes: In class (1), we modify the DMRG sweeping procedure [37] to pick one of the excited eigenstates of the effective Hamiltonian at each step and hence arrive at an excited eigenstate of the full Hamiltonian. We call this algorithm Excited State-DMRG (ES-DMRG). In class (2), we target a specific energy λ by repeatedly applying the operator $(H-\lambda)^{-1}$ to the state vector. We call this algorithm shift-and-invert MPS (SIMPS).

Throughout this manuscript, we use the following one-dimensional Hamiltonian

$$H = \sum_i \vec{S}_i \cdot \vec{S}_{i+1} + \sum_i h_i S_i^z \tag{1}$$

where h_i are sampled uniformly from $[-W, W]$, which is known to have the entire many-body spectrum become localized for $W \gtrsim 3.5$ [7, 21].

Excited state DMRG: The first of these algorithms, while conceptually interesting, is simple to describe and has the advantage of requiring minimal modifications to a current DMRG code. A standard DMRG code sweeps over sites; when working on site i, an effective Hamiltonian H_i is generated which involves tracing over the other auxiliary and physical degrees of freedom. This effective Hamiltonian H_i is then diagonalized and the parameters on site i of the MPS are replaced with the ground state of H_i. In our new approach, instead of considering only the ground state of H_i we consider all its eigenvalues (of which there are pM^2 where M is the bond-dimension and p the physical dimension) replacing the parameters of site i with one of these eigenvalues. In particular, we select the eigenvalue with energy closest to the energy of the current MPS to minimize the amount of change in the state as our algorithm progresses. We then follow the typical approach of sweeping back and forth through all the sites.

As in normal DMRG, we find that a proper starting

configuration and bond-dimension protocol can enhance the efficiency of the algorithm keeping it from being stuck and allowing it to more widely sample excited states. In particular, we start with the algorithm in a product state in the S_z basis of bond-dimension two and slowly ramp up the bond-dimension increasing it by one every few sweeps. This ensures we find low bond-dimension states at the energy at which the algorithm converges. From these sweeps, we take the state we find with lowest variance. This algorithm scales as typical DMRG. While currently we are exactly diagonalizing the effective Hamiltonian, a standard shift-and-invert procedure would allow the eigenstate of the effective Hamiltonian to be found without a full diagonalization. While this approach is powerful, it has the undesirable property of not having a clean way to target a particular energy.

Shift and Invert MPS (SIMPS): Our goal is to target a particular energy λ. The shift-and-invert technique [21] inverts a spectrum by repeatedly applying $(H-\lambda)^{-1}$ to a random state to converge to an eigenstate with eigenvalue near λ. We develop an analogous approach in the MPS language called SIMPS. Starting with a random MPS, we iteratively apply $(H-\lambda)^{-1}$ until we reach an MPS that well approximates an eigenstate close to λ.

The key to SIMPS is the development of an inverse-DMRG approach which, given an MPO O (in our case $O=(H-\lambda)$) and MPS $|\psi\rangle$, applies $O^{-1}|\psi\rangle$. However, inverting an MPO directly is not practical as (1) there is no known efficient algorithm for accurately inverting an MPO and (2) the output of such an algorithm would require bond dimension significantly larger than what is required to describe a single eigenstate. The more efficient alternative is to construct a MPS $|\varphi\rangle$ which variationally approaches $O^{-1}|\psi\rangle$. We accomplish this task by varying φ in order to minimizing the distance $\||O|\varphi\rangle-|\psi\rangle\|^2$ between $|\psi\rangle$ and $O|\varphi\rangle$. Specifically, we obtain the following variational prescription

$$\frac{\partial}{\partial\varphi^*_{i,\sigma}}\langle\varphi|O^\dagger O|\varphi\rangle=\frac{\partial}{\partial\varphi^*_{i,\sigma}}\langle\varphi|O^\dagger|\psi\rangle, \tag{2}$$

where $\partial/\partial\varphi^*_{i,\sigma}$ indicates the variation of the MPS representation of $\langle\varphi|$ by varying the matrix $\varphi^*_{i,\sigma}$ on site i and spin σ. Eq. (2) is described pictorially in Fig. 1. To update the matrices at a particular site, one needs to solve a linear equation problem that involves a dense, symmetric, and semi positive-definite matrix. To optimize the entire MPS $|\varphi\rangle$, one needs to sweep back and forth over the sites as in standard DMRG. One can either replace the ψ after each site or after a number of sweeps. While the former is significantly faster in practice, the convergence of the latter is mathematically well controlled and the data presented here uses that version unless otherwise noted.

Precision of this method is controlled by the bond dimension of the MPS $|\varphi\rangle$. The computationally dominant piece is in solving the dense system of linear equations

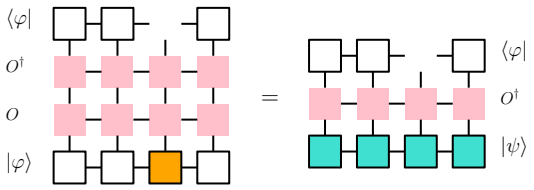

FIG. 1. Pictorial representation for optimizing $\||O|\varphi\rangle-|\psi\rangle\|^2$. Here as an example, we consider optimizing the third site (colored orange) for a $L=4$ chain. The MPO O (pink) and the MPS $|\psi\rangle$ (cyan) are given. To update the orange block, we solve a linear equation, treating the orange block as an unknown vector x; the other part of the network on the left hand side, after being contracted, amounts to a symmetric semi positive-definite matrix A, and the matrices on the right hand side of the equation becomes a known vector b. The entire MPS is optimized by sweeping.

which scales as $O(L(pM^2)^3)$ using a direct solver and as $O(L(pM^2)^2)$ when using an iterative solver, where p is the number of physical degrees of freedom per site, and M is the maximum bond dimension of the MPS.

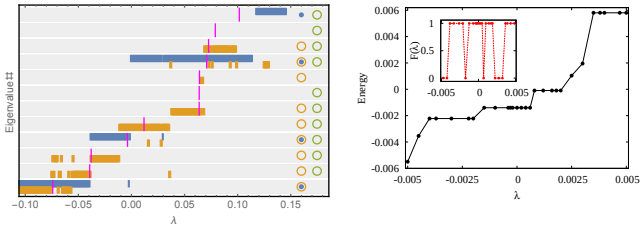

FIG. 2. (left) Convergence to eigenstates 503-514. Magenta lines indicate the twelve eigenvalues in this range. SIMPS: Blue and yellow bars indicate the basins of convergence, as a function of parameter λ, found for two random MPS initial conditions. Yellow and blue dots indicate whether sweeps of the two respective initial conditions find a given eigenvalue. ES-DMRG: Green dots indicate whether ES-DMRG found the eigenvalue after being run with 6144 random product state initial conditions (right) Energy vs λ for $L=30, W=10$. 29 MPSs obtained using SIMPS with $M=40$ are displayed on this plot, with 8 distinct energies. Inset: Fidelity function $F(\lambda_i)=|\langle MPS(\lambda_i)|MPS(\lambda_{i+1})\rangle|$. $F(\lambda)$ also shows 8 distinct states, and matches exactly with the energy curve.

Generating Eigenstates: We start by producing eigenstates at length $L=10$ such that they can be compared with ED. Here, for both algorithms, we consider a fixed disorder configuration with $W=8$ and artificially limit bond dimension to $M=12$. Since ES-DMRG can't target particular energies, we run the algorithm many times verifying that the energies it finds match those of the true Hamiltonian (see Fig. 2). In SIMPS, we have a tunable shift parameter λ and focus on the energy window of $\lambda\in[-0.1,0.1]$, within which there are 12 eigenstates as shown by ED. When running at a limited bond dimension with fixed initial conditions, the SIMPS algo-

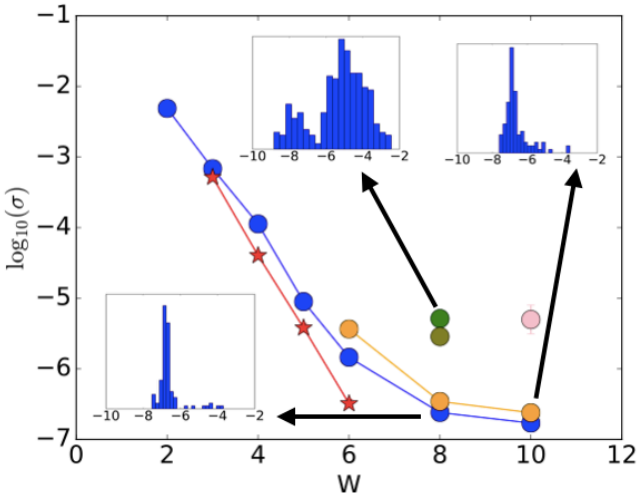

FIG. 3. Values of $\langle \log_{10}(\sigma) \rangle$ for various algorithms and parameters at different disorder strengths W. Blue line ($L = 30$) and orange line ($L = 40$) are SIMPS runs at $M = 60$ with λ tuned exactly to the middle of the spectrum for each disorder realization, where the lowest and highest eigenvalues are obtained via DMRG and the disorder configurations are the same scaled pattern at different W for $L = 30$ and $L = 40$, respectively. Values of $W \leq 5$ are not necessarily reliably converged. Green point is ES-DMRG at $M = 20$, $L = 30$ and pink point is ES-DMRG at $M = 20$, $L = 100$. The dark green point is SIMPS at $M = 20$, $L = 30$ showing that ES-DMRG and SIMPS converge to similar accuracy at the same bond dimension and chain length. Red line is SIMPS $M = 200$, $L = 30$ computed using the faster sweeping. Insets are distributions of σ at the respective parameters.

rithm does not always hit the targeted eigenstate. Remarkably, it does find an eigenstate near the desired energy with high fidelity; for $L = 10, M = 12$ we never see a situation where the fidelity is less then 10^{-5}. Fig. 2 shows the eigenvalues identified during a λ sweep for different initial conditions and bond-dimensions of SIMPS.

We verify the found eigenstates aren't biased toward low entanglement by comparing histograms of entanglement entropies for eigenstates generated using ED to those generated using SIMPS and ES-DMRG at artificially reduced bond-dimension M=12 (figure included in the supplementary material).

Another useful metric to quantify the quality of eigenstates is $\sigma = \sqrt{\langle H \rangle^2 - \langle H^2 \rangle}$. Note that while a true eigenstate has $\sigma = 0$, numerically calculated standard deviations are limited by machine precision (due to the square root the limit is one part in $\sim 10^7$).

We find that, using SIMPS at $M = 60$, we can obtain eigenstates of chains of length $L = 30, 40$ and $W = 8$ with values of $\langle \sigma \rangle$ peaked at machine precision (see fig. 2). These tests are conducted for the worst case scenario – we target λ exactly to the middle of the energy spectra (lowest and highest energies calculated by DMRG) where the many-body density of states is near maximum. Running ES-DMRG at $M = 20$ for chains with $\{L = 30, W = 8\}$ and $\{L = 100, W = 10\}$, we find approximate eigenstates with $\langle \log_{10}(\sigma) \rangle$ somewhat larger than SIMPS. For long chains, the inter-level spacing is smaller then the σ which can be resolved by machine precision and we develop, in the supplemental material, an additional metric to validate these states.

Many-body localization in large systems: We now use the tools that we have developed to test, in a previously inaccessible regime of long chains, three key properties of MBL matter: failure to thermalize, low entanglement entropy of highly excited eigenstates, and the existence of a large number of local excitations.

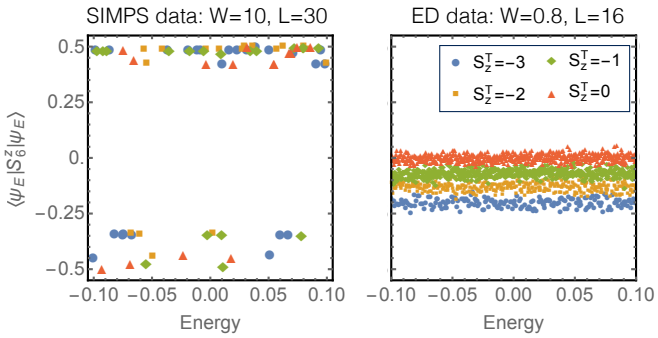

FIG. 4. *Left:* Site value of $\langle S_z^6 \rangle$ as a function of energy at $L = 30$ for a fixed disorder configuration with disorder strength $W = 10$. Eigenstates are obtained using SIMPS, with $M = 40$. Note the small energy range. The energy scan was performed with 200 λ evenly spaced in $[-0.1, 0.1]$. In the $S_z^T = -3, -2, -1, 0$ sectors, a total of 74 distinct MPSs were found. *Right:* Site value of $\langle S_z^6 \rangle$ for $L = 16, W = 0.8$ generated using ED.

The eigenstate thermalization hypothesis (ETH) states that in thermalized quantum systems nearby eigenstates have similar expectation values of local observables [38–40]. We test this by computing the expectation value of a representative local observable $\langle S_6^z \rangle$ for two chains: one with $L = 16$ at $W = 0.8$ (expected to obey ETH) and another with $L = 30$ at $W = 8$ (expected to violate ETH). Specifically, we choose eigenstates from a *small energy window* in the range $[-0.1, 0.1]$. We also filter the eigenstates by total $S_z^T = \sum_i S_i^z$. For the case $W = 8$, SIMPS discovered 74 eigenstates that were close in energy (but not consecutive). As shown in Fig. 4, the corresponding $\langle S_6^z \rangle$ vary wildly confirming the violation of ETH. On the other hand, for $W = 0.8$ ETH prevails – $\langle S_6^z \rangle$ lies in a narrow band, with the position of the band depending on the global conserved quantity S_z^T [see Fig. 4].

The second key property that we investigate is the mid-bond entanglement entropy of highly excited eigenstates. In Fig. 4 we plot the mean mid-bond entanglement entropy as a function of disorder strength for chains of length $L = 14$ (ED) and $L = 30, 40$ (SIMPS). We ob-

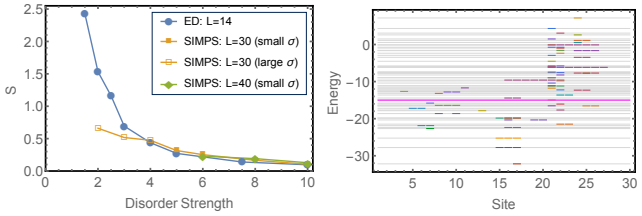

FIG. 5. (left) Dependence of mid-bond entanglement entropy S on the disorder strength for various chain lengths. 50 disorder realizations were used for $L = 14$ and 100 for $L = 30$ and $L = 40$. Open markers indicate points at low disorder strengths for which SIMPS failed to obtain states with low standard deviation of the energy. For SIMPS we set $M = 60$ and tuned λ to the exact middle of the eigenspectrum for each disorder realization. This saturation confirms entanglement in the MBL is independent of system size. (right) Spectrum of 62 excitations (colored bars) produced by local modifications of a reference MPS eigenstate (long magenta line). The horizontal axis marks the site on which the MPS is being modified. Bars of the same color correspond to the same excitation as determined by their energies. [$L = 30$, $W = 10$, $M = 15$, excited eigenstates all have $\sigma < 0.0005$].

serve that for $W > 4$ the mid-bond entanglement entropy is essentially independent of system size, thus confirming the predicted saturation in the MBL phase. On the other hand for $W < 4$ the ED and SIMPS data strongly disagree. We attribute this disagreement to the failure of SIMPS to find high quality eigenstates in this near-ergodic and ergodic regime as demonstrated in Fig. 3.

The third property that we investigate is the existence of a large number of local excitations of the system. In Fig. 5 we show a spectrum of these local excitations constructed with respect to an eigenstate at $E = -15.002$. To construct a local excitation on a given site, we take the following steps. (1) We bring the reference state to canonical form with respect to the target site. (2) We obtain the effective Hamiltonian on the target site. (3) We construct an MPS for *all* eigenstates of the effective Hamiltonian on the target site. (4) Most of the MPSs produced in step (3) are superpositions of a large number of local excitations, and hence are not necessarily good eigenstates. Therefore, we retain only the MPSs that have a low σ. Surprisingly, even after the filtering step, we find a large number of local excitations (there are 62 distinct ones in Fig. 5).

Outlook: In our manuscript, we have presented two algorithms ES-DMRG and SIMPS for finding matrix product state representations of interior eigenstates.

We are particularly excited about two potential consequences of our work for many-body localization. First, as demonstrated in Fig. 5, the algorithms that we have developed seem to work right up to the localization-delocalization transition suggesting these algorithms can be used to probe the transition from the localized side [41]. Second, it seems possible that by collating and orthogonalizing the "local excitation" data of Fig. 5 one can construct and characterize the local integrals of motion that are central the many-body localization phenomenology.

We believe that the methods that we have developed are not limited to the study of strongly-localized matter. Specifically, these methods have the potential to be significantly better for finding low-lying excited states of conventional Hamiltonians as compared to current state of the art methods – an extremely important problem both in quantum chemistry and condensed matter physics. Moreover, we suspect that further improvements can be made to our algorithms by applying more sophisticated diagonalization methods to matrix product states.

Note Added: During the preparation of this manuscript we became aware of two independent works that also developed an algorithm similar to ES-DMRG for finding excited eigenstates in MBL systems [42] and molecular systems [43].

Acknowledgements: The authors thank Hitesh J. Changlani, Victor Chua, David Huse, Vedika Khemani, Vadim Oganesyan, Shivaji Sondhi, and Gil Refael for helpful discussions. Computations for all points in this work were done on codes we developed except for the $M = 200$, $L = 30$ points in Fig. 3 which were computed on an implementation of SIMPS that we built on top of the ITensor Library [44]. We acknowledge MPI-PKS and the Aspen Center for Physics for their hospitality. This research is part of the Blue Waters sustained-petascale computing project, which is supported by the National Science Foundation (award number ACI 1238993) and the state of Illinois. Blue Waters is a joint effort of the University of Illinois at Urbana-Champaign and its National Center for Supercomputing Applications. DP acknowledges support from the Charles E. Kaufman foundation; BKC and XY acknowledges support from grant DOE, SciDAC FG02-12ER46875.

[1] P. W. Anderson, Phys. Rev. **109**, 1492 (1958).
[2] L. Fleishman and P. W. Anderson, Phys. Rev. B **21**, 2366 (1980).
[3] B. L. Altshuler, Y. Gefen, A. Kamenev, and L. S. Levitov, Phys. Rev. Lett. **78**, 2803 (1997).
[4] D. M. Basko, I. L. Aleiner, and B. L. Altshuler, Annals of Physics **321**, 1126 (2006).
[5] D. M. Basko, I. L. Aleiner, and B. L. Altshuler, Phys. Rev. B **76**, 052203 (2007).
[6] V. Oganesyan and D. A. Huse, Phys. Rev. B **75**, 155111 (2007).
[7] A. Pal and D. A. Huse, Phys. Rev. B **82**, 174411 (2010).
[8] I. L. Aleiner, B. L. Altshuler, and G. V. Shlyapnikov, Nat. Phys. **6**, 900 (2010).
[9] C. Monthus and T. Garel, Phys. Rev. B **81**, 134202 (2010).
[10] J. Z. Imbrie, "On many-body localization for quantum

spin chains," (2014), 1403.7837.
[11] R. Nandkishore and D. A. Huse, Annual Review of Condensed Matter Physics **6**, 15 (2015).
[12] B. Bauer and C. Nayak, Journal of Statistical Mechanics: Theory and Experiment **2013**, P09005 (2013).
[13] M. Serbyn, Z. Papić, and D. A. Abanin, Phys. Rev. Lett. **111**, 127201 (2013).
[14] D. A. Huse, R. Nandkishore, and V. Oganesyan, Phys. Rev. B **90**, 174202 (2014).
[15] V. Ros, M. Müller, and A. Scardicchio, Nuclear Physics B **891**, 420 (2015).
[16] R. Vosk and E. Altman, Phys. Rev. Lett. **110**, 067204 (2013).
[17] R. Vosk and E. Altman, Phys. Rev. Lett. **112**, 217204 (2014).
[18] D. Pekker, G. Refael, E. Altman, E. Demler, and V. Oganesyan, Phys. Rev. X **4**, 011052 (2014).
[19] R. Vosk, D. A. Huse, and E. Altman, "Theory of the many-body localization transition in one dimensional systems," (2015), 1412.3117.
[20] A. C. Potter, R. Vasseur, and S. A. Parameswaran, "Universal properties of many-body delocalization transitions," (2015), 1501.03501.
[21] D. J. Luitz, N. Laflorencie, and F. Alet, Phys. Rev. B **91**, 081103 (2015).
[22] T. C. Berkelbach and D. R. Reichman, Phys. Rev. B **81**, 224429 (2010).
[23] S. Iyer, V. Oganesyan, G. Refael, and D. A. Huse, Phys. Rev. B **87**, 134202 (2013).
[24] J. A. Kjall, J. H. Bardarson, and F. Pollmann, Phys. Rev. Lett. **113**, 107204 (2014).
[25] M. Žnidarič, T. Prosen, and P. Prelovšek, Phys. Rev. B **77**, 064426 (2008).
[26] J. H. Bardarson, F. Pollmann, and J. E. Moore, Phys. Rev. Lett. **109**, 017202 (2012).
[27] M. Serbyn, Z. Papić, and D. A. Abanin, Phys. Rev. Lett. **110**, 260601 (2013).
[28] A. Chandran, I. Carrasquilla, Kim, D. Abanin, and G. Vidal, arXiv:1410.0687 (2014).
[29] D. Pekker and B. K. Clark, "Encoding the structure of many-body localization with matrix product operators," (2014), 1410.2224.
[30] F. Pollmann, V. Khemani, J. I. Cirac, and S. L. Sondhi, "Efficient variational diagonalization of fully many-body localized hamiltonians," (2015), 1506.07179.
[31] C. D'Errico, E. Lucioni, L. Tanzi, L. Gori, G. Roux, I. P. McCulloch, T. Giamarchi, M. Inguscio, and G. Modugno, Phys. Rev. Lett. **113**, 095301 (2014).
[32] C. Meldgin, U. Ray, P. Russ, D. Ceperley, and B. DeMarco, "Probing the bose-glass–superfluid transition using quantum quenches of disorder," (2015), 1502.02333.
[33] M. Schreiber, S. S. Hodgman, P. Bordia, H. P. Lüschen, M. H. Fischer, R. Vosk, E. Altman, U. Schneider, and I. Bloch, Science **349**, 842 (2015), http://www.sciencemag.org/content/349/6250/842.full.pdf.
[34] B. Swingle, arXiv:1307.0507 (2013).
[35] M. Friesdorf, A. H. Werner, W. Brown, V. B. Scholz, and J. Eisert, arXiv:1409.1252 (2014).
[36] S. R. White, Phys. Rev. Lett. **69**, 2863 (1992).
[37] U. Schollwöck, Annals of Physics **326**, 96 (2011).
[38] J. M. Deutsch, Phys. Rev. A **43**, 2046 (1991).
[39] M. Srednicki, Phys. Rev. E **50**, 888 (1994).
[40] M. Rigol, V. Dunjko, and M. Olshanii, Nature **452**, 854 (2008).
[41] T. Grover, "Certain general constraints on the many-body localization transition," (2014), 1405.1471.
[42] V. Khemani, F. Pollmann, and S. L. Sondhi, "Obtaining highly-excited eigenstates of many-body localized hamiltonians by the density matrix renormalization group," (2015), 1509.00483.
[43] W. Hu and G. K. Chan, Journal of Chemical Theory and Computation (2015).
[44] E. M. Stoudenmire and S. R. White, http://itensor.org/.